The effect of pressure on the Raman spectra of solids. VII. The internal Raman bands in solid and coordinated pyridine

A. M. Heyns and M. W. Venter

Citation: The Journal of Chemical Physics **93**, 7581 (1990); doi: 10.1063/1.459389
View online: http://dx.doi.org/10.1063/1.459389
View Table of Contents: http://scitation.aip.org/content/aip/journal/jcp/93/11?ver=pdfcov
Published by the AIP Publishing

The effect of pressure on the Raman spectra of solids. VII. The internal Raman bands in solid and coordinated pyridine

A. M. Heyns and M. W. Venter
Department of Chemistry, University of Pretoria, 0002 Pretoria, South Africa

(Received 27 September 1989; accepted 31 July 1990)

The pressure dependences of the internal Raman-active modes of solid pyridine and pyridine-d_5 in both the crystalline and glassy modifications as well as of the complexes $Zn(py)_2Cl_2$, $Ni(py)_2Cl_2$, and $Ni(py)_4Cl_2$ are reported. When pyridine is frozen by the application of pressure, some ring modes as well as those involving the hydrogen atoms reflect this transformation. Upon the coordination of pyridine to metal ions, the ring vibrations show appreciable blue shifts. The pressure dependences of ν_1, the C–C stretching mode, and ν_{12}, the in-plane ring bending mode of the pyridine rings, are discussed in detail. The unusually high d_5–h_5 isotopic ratio of ν_{12} and its contrasting pressure dependences in the liquid and condensed phases of pyridine-d_5 are explained. The association of pyridine molecules in the condensed phase does not occur through hydrogen bonds and the C–H stretching modes, in particular, show that repulsive intermolecular forces become very significant at higher pressures. The ratio of the intensities $I\nu_{12}/I\nu_1$ varies linearly with the strength of the M–N bonds in a series of pyridine complexes and a correlation also exists between $I\nu_{12}/I\nu_1$ and $\partial\nu_{12}/\partial p$. The vibrations ν_1 and ν_2 are coupled through Fermi resonance in pyridine and its complexes and the pressure dependence of the Fermi resonance constant W is calculated for $Zn(py)_2Cl_2$. The C–H stretching modes reflect the presence of more than one distinct pyridine group in the lattice and are of much lower intensity than in complexes where only one distinct pyridine group is found.

I. INTRODUCTION

Pyridine is a polar molecule with a dipole moment of 2.20 D and can thus be expected to be associated in the liquid state.[1] This association between pyridine molecules in various solvents,[1,2] the adsorption of pyridine onto metal surfaces[3,4] as well as the bonding between pyridine and various metal ions,[5–11] have been widely reported in the literature. High-pressure Raman spectra of liquid pyridine, of pyridine dissolved in various solvents,[1,2] of solid pyridine,[12] and of pyridine adsorbed on colloidal gold particles[13] have also been published. These results indicated that pyridine in solution is largely associated in dimeric complexes and that a ring hydrogen is involved in this self-association.[1,2] On the other hand, the high-pressure Raman spectra of solid pyridine did not provide any evidence of the existence of strong hydrogen bonds in the condensed state.[12] Surface-enhanced Raman spectra of adsorbed pyridine on gold particles were interpreted in terms of a weakly chemisorbed molecule which is bonded by means of the lone pair of electrons on the nitrogen atom to Lewis acid sites on the metal.[13] There were also indications of different pyridine conformations near the surfaces and/or of inequivalent adsorption sites.[13] The high-pressure Raman spectra of pyridine were, with the exception of our earlier results,[12] confined to a study of the ring modes ν_1 and ν_{12} of pyridine. The only pyridine coordination compound that has been thoroughly studied by means of high-pressure Raman spectroscopy is $Zn(py)_2Cl_2$.[6,14]

In the present paper, the internal Raman-active pyridine modes at high pressures of solid pyridine and pyridine-d_5 in the crystalline and glassy states are compared with those of the distorted octahedral complex $Ni(py)_4Cl_2$, the polymeric octahedral complex $Ni(py)_2Cl_2$, and the distorted tetrahedral complex $Zn(py)_2Cl_2$. The more specific aims of this study were to investigate the intermolecular forces between the pyridine rings in the condensed phase of pyridine and to throw more light on the Fermi resonance which occurs between the ring modes ν_1 and ν_{12} in all the compounds studied here. Finally, the influence of the strength of N–M bonding and possible N– – –H interactions on the Raman spectra over a wide pressure range will be reported.

II. EXPERIMENTAL

Details regarding the Raman spectrometer and diamond anvil cell used have already been published.[12] The pyridine used in the high-pressure measurements was purified by refluxing over KOH for a minimum period of time of 24 h and then distilling it fractionally. Only the fraction obtained at 110 °C was used and the diamond anvil cell was immediately loaded with a sample of this fraction.

All the complexes used in these investigations were isolated from ethanolic solutions of pyridine and MCl_2 (M = Ni, Cu, Cd, Zn). These products were isolated from ethanol, dried under vacuum, and stored in a dessicator over P_2O_5. The C, H, N, and metal analyses were all determined to be within 0.5% of the calculated values.

III. CRYSTAL STRUCTURES AND POLYMORPHISM

It was reported earlier[12] that pyridine freezes at approximately 10 kbar at ambient temperatures and that the crystalline modification undergoes a phase transition at ~20 kbar. These results have been confirmed by Zakin *et al.*[1] The

 0021-9606/90/237581-11$03.00

high-pressure Raman spectra of pyridine have also been reported elsewhere,[15] however, these results do not entirely agree with ours[12] or those of Zakin *et al.*[1]

When pyridine is frozen by the application of pressure, a glassy phase can also be formed.[12,15] The lattice modes of the latter modification differ significantly from those of the crystalline phase, but the internal modes are quite similar, also closely resembling those of the liquid. The four independent pyridine molecules predicted under the space group $Pna2_1(C_{2v}^9)$ with $Z = 16$[16] are not reflected in the internal Raman-active modes of crystalline pyridine.[12] In this complicated crystal structure, which is antiferroelectric, eight molecular dipoles are aligned almost parallel to the a axis and the remaining eight parallel to the b axis. In assuming a more symmetrical structure[16] under the space group $Pccn(D_{2h}^{10})$, the number of distinct pyridine groups is reduced from four to two, corresponding to the two orientations mentioned above. If factor group splittings are ignored, each internal pyridine mode can be doubled corresponding to the two independent groups. It was previously reported[12] that a limited number of bands of solid pyridine-d_5 are split into two components, such as ν_1, ν_{9a}, and ν_{12}, and this could possibly be interpreted in terms of the existence of two independent pyridine rings.

The crystal structure of pseudotetrahedral $Zn(py)_2Cl_2$ is given by the space group $P2_1/c(C_{2h}^5)$ with $Z = 4$.[17] Two types of pyridine rings are present in this structure, i.e., those forming dimer-like pairs and those forming an infinite column in the crystal. All of the internal pyridine modes can therefore be expected to be split into two components. $Zn(py)_2Cl_2$ undergoes a phase transition at ~ 10 kbar[6] and is most probably converted into a polymeric octahedral structure.[18]

Polymeric octahedral $Ni(py)_2Cl_2$ is assumed to have the same crystal structure as $Cu(py)_2Cl_2$ and $Cd(py)_2Cl_2$.[19,20] These compounds belong to the monoclinic space group $P2_1/n(C_{2h}^5)$ with $Z = 2$. Only one distinct pyridine ring is found in this structure. On the other hand, the pseudo-octahedral complex $Ni(py)_4Cl_2$ belongs to the tetragonal space group $I4_1/acd(D_{4h}^{20})$ with $Z = 8$.[21] The site symmetry of the Ni ions is D_2 and with four ions per primitive unit cell, the N atoms of the pyridine rings and the Cl atoms all occupy sites of C_2 symmetry. These sites can only contain 8 groups and this means that the eight chlorine atoms, one group of eight pyridine rings, and another group of eight pyridine rings all occupy sites of C_2 symmetry in the primitive unit cell. Just as in the cases of solid pyridine and phase II of $Zn(py)_2Cl_2$, the Raman-active modes of $Ni(py)_4Cl_2$ could be split into two components. The undistorted $Ni(py)_4Cl_2$ of D_{4h} symmetry in the "free" state does possess the stereochemical arrangement which allows d_π-electron delocalization between the metal ion orbitals and the π electrons of the pyridine rings. Such an interaction will be controlled by the d_π-electron delocalization from the nickel ion to the π^* orbitals of the coordinated pyridine rings. Octahedral complexes of Ni(II) are commonly found; this is, however, not so with mixed complexes of the general formula NiX_4Y_2, where X is a stronger ligand that Y.[22] The energy change associated with conversion of a diamagnetic square planar NiX_4^{2+} complex to a paramagnetic "octahedral" complex NiX_4Y_2 is > 0.[22] It will therefore be interesting to see whether the Raman bands of $Ni(py)_4Cl_2$ reflect any d_π-electron delocalization from Ni to the π^* orbitals of pyridine, since $Ni(py)_4Cl_2$ is expected to be stabilized accordingly in order to exist at all. The effect of pressure, if any, on this stabilization is also of interest and will be reported in the present study.

IV. RESULTS

The Raman spectra of crystalline pyridine and $Ni(py)_2Cl_2$ are shown in Figs. 1 and 2, respectively. These results, in addition to those of pyridine-d_5, $Zn(py)_2Cl_2$ (phases I and II), and $Ni(py)_4Cl_2$ are summarized in Table I. Only a very limited number of internal Raman bands reflect the presence of two or more crystallographically distinct pyridine groups in the lattices of pyridine, pyridine-d_5, $Ni(py)_4Cl_2$, and $Zn(py)_2Cl_2$. The shifts in the Raman frequencies between liquid and solid pyridine and solid and coordinated pyridine are summarized in Table II. The assignment of the modes summarized in Table I was done by reference to other studies involving pyridine and its complexes,[1-12] by considering d_5/h_5 isotopic shifts in the modes of solid pyridine and also be observing significant frequency shifts in the pyridine ring modes upon coordination to metal ions.

The molecular interactions that occur in pyridine dissolved in various solvents have been well-documented.[1,2] In analyzing the Raman spectra summarized in Table I, the perturbations arising from these interactions must be taken into account. The shifts that occur because of changes in the energy levels, lifetimes of the relevant states that change line shapes and affect bandwidths, and the changes in the intensities brought about by the distortion of the molecules are all indications of the effects of molecular interactions.

The molecular interactions in pyridine also include hydrogen bonding between a nitrogen atom and a C–H group, π–π bonding involving the aromatic rings, and polar interactions.[1] Any major differences between the molecular interactions of liquid and solid pyridine should be clearly evident in their Raman bands. On the other hand, the differences in the two solid state modifications of condensed pyridine, which

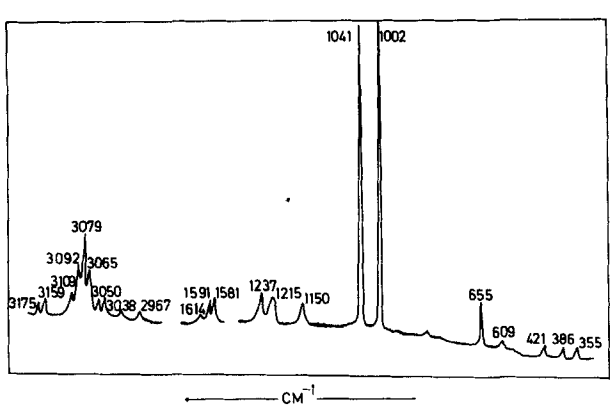

FIG. 1. The Raman spectrum of condensed pyridine at 19 kbar.

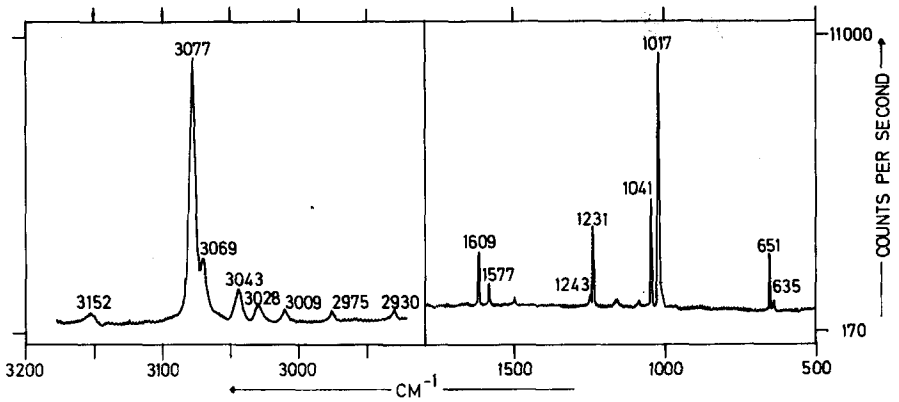

FIG. 2. The Raman spectrum of $Ni(py)_2Cl_2$ at ambient conditions.

are clearly evident in the lattice modes of these compounds,[12] can possibly also be reflected in the internal pyridine modes.

In the following discussion of the high-pressure Raman results, the results obtained for the different classes of modes will be dealt with separately.

A. Ring modes

It is seen in Table II that the ring modes of pyridine such as ν_1, ν_{6a}, ν_{8a}, and ν_{12} are shifted to the blue upon coordination to the metal ions. When the Raman bands in liquid and condensed pyridine are compared, blue shifts also occur in

TABLE I. Frequencies of assignments of the Raman-active vibrations in pyridine, pyridine-d_5, $Zn(py)_2Cl_2$ (phases I and II), $Ni(py)_2Cl_2$, and $Ni(py)_4Cl_2$ (dv/dP values are shown in brackets).

Mode	Species	Description	Pyridine[a,b]	Pyridine-d_5	d_5/h_5	$Zn(py)_2Cl(II)$	$Zn(py)_2Cl_2(I)$[a]	$Ni(py)_2Cl_2$	$Ni(py)_4Cl_2$
ν_1	A_1	C–C ring stretch	998*vs*(0.37)	971*vs*/978*w*(0.31)	0.97/0.98	1023*vs*(0.5)	1027*vs*(0.5)	1017*vs*(0.40)	1011*vs*/999*w*(0.6)
ν_2	A_1	C–H stretch	3070*vs*(0.86)}	2300*vs*(0.90)}	0.75	3076*vs*(0.82)	3085*vs*(1.0)	3077*m*(0.73)	3075*m*(0.86)
			3081*w*(0.96)}	2308*s*(0.90)}		3086*sh*(1.27)			3054*m*(0.81)
ν_3	B_2	In-plane H bend	1233*w*(0.42)	···	···	1243*w*}(0.67)	1258*vw*(0.29)	1243*vw*	1235*m*
						1247*w*}			
ν_4	B_1	Out-of-plane ring bend	···	···	···	···	···	···	···
ν_5	B_1	Out-of-plane H bend	1010*vw*(0.43)	843*m*(0.51)	0.83	1001*sh*	1000sh	···	1000*sh*
ν_{6a}	A_1	In-plane ring bend	609*vw*	586*w,br*	0.96	646*vw*(~0)	···	635*w*	627*w*
ν_{6b}	B_2	In-plane ring bend	653*w*	625*w*(0.43)	0.96	650*m*(~0)	658*m*	651*m*	669*m*(0.1)
ν_{7a}	A_1	Out-of-plane bend	···	···	···	···	···	···	···
ν_{7b}	B_2	Out-of-plane bend	···	···	···	···	···	···	···
ν_{8a}	A_1	C–C ring stretch	1588(0.30)	1559*w*(0.28)	0.98	1612*m*(0.20)	1612*m*	1609*m*	···
ν_{8b}	B_2	C–C ring stretch	1577(0.37)	1544*m*(0.26)	0.98	1577*w*(0.10)	1581*w*	1577*m*(0.45)	1570*m*
ν_{9a}	A_1	In-plane H bend	1213*w*(0.40)	893*w*(0.48)	0.72	1217*w*(~0)	1210*w*	···	1217*m*
ν_{9b}	B_2	In-plane H bend	···	900*w*(0.48)		1226*m*(~0)	···	1231*m*	···
ν_{10a}	A_2	Out-of-plane H bend	849*vw*(0.54)	720*w,br*	0.78	···	···	···	···
ν_{10b}	B_1	Out-of-plane H bend	~960*vw*(0.26)	778*w*	0.81	···	···	···	···
ν_{11}	B_1	Out-of-plane bend	···	···	···	···	···	···	···
ν_{12}	A_1	In-plane ring bend	1038*vs*(0.35)	1015*w*/1006(0.33)	0.98	1048*w*(0.10)	1050(0.20)	1041*m*(0.20)	1037*m*(0.18)
ν_{13}	A_1	C–H stretch	···	···	···	···	···	···	···
ν_{14}	B_2	C–C ring stretch	···	···	···	···	···	···	···
ν_{15}	B_2	In-plane H bend	1150*w*(0.58)	870*vw*	0.76	~1165*vw*(~0)	1165*vw*(0)	1155*vw*	1142*vw*(~0)
ν_{16a}	A_2	Out-of-plane ring bend	384*w*(0.10)	···	···	···	···	···	388*w*
ν_{16b}	B_1	Out-of-plane ring bend	417*w*(0.36)	···	···	425*w*	···	···	···
ν_{17a}	A_2	Out-of-plane H bend	986*vw*	···	···	···	···	···	980*vw*
ν_{17b}	B_1	Out-of-plane H bend	1010*w*(0.55)	···	···	1003*w*(~0)	···	···	···
ν_{18a}	A_1	In-plane H bend	1068*vw*	824*w,br*(0.54)	0.77	1072*vw*	···	···	1073*vw*
ν_{18b}	B_2	In-plane H bend	1068*vw*	843*w*(0.43)	0.79	···	···	···	1060*w*
ν_{19a}	A_1	C–C ring stretch	···	···	···	···	···	···	···
ν_{19b}	B_2	C–C ring stretch	···	···	···	···	···	···	···
ν_{20a}	A_1	C–H ring stretch	3061*w*/3100*sh*(0.46)	2260/2272	0.74	3083*sh*(0.43)	3075*sh*(0.61)	3069*sh*	3067*sh*
ν_{20b}	B_2	C–H ring stretch	···	2284/2296	···	···	···	···	···

[a] At 11 kbar.
[b] Reference 12.

TABLE II. The frequency shifts of some Raman-active internal modes of liquid pyridine upon crystallization at 10 kbar and of liquid and solid pyridine upon coordination to Ni(II) and Zn(II).[a]

Mode	$\Delta\nu$, liq→solid	$\Delta\nu$, liq→complex			$\Delta\nu$, solid→complex		
		$Zn(py)_2Cl_2$	$Ni(py)_2Cl_2$	$Ni(py)_4Cl_2$	$Zn(py)_2Cl_2$	$Ni(py)_2Cl_2$	$Ni(py)_4Cl_2$
ν_1, (C–C) ring stretch	7	32	26	20	25	19	13
ν_2, (C–H) stretch	13	15	20	18	2	7	5
ν_3, in-plane H bend	6	0	4	8	−6	−2	2
ν_{6a}, in-plane ring bend	5	42	31	23	37	26	18
ν_{6b}, in-plane ring bend	0	1	−2	−4	1	−2	−4
ν_{8a},(C–C) ring stretch	6	30	29	20	24	23	14
ν_{8b}, (C–C) ring stretch	3	3	4	−4	0	1	−7
ν_{9a}, in-plane H bend	16	9	16	>18	−7	0	−16
ν_{12}, in-plane ring bend	7	17	12	6	10	5	−1
ν_{15}, in-plane H bend	3	18	···	−5	15	5	−8
ν_{18a}, in-plane H bend	−1	3	···	4	4	···	5

[a] $\Delta\nu$ is the shift in frequency upon freezing or coordination. liq—liquid pyridine, solid—solid pyridine.

these modes, however, they are significantly smaller, particularly if it is borne in mind that the frequencies of liquid pyridine at ambient pressures are compared with those of the solid at 10 kbar.

The A_1-ring modes ν_1 and ν_{12} (under C_{2v} symmetry for free pyridine) are shown in Fig. 3. The pressure dependences of the internal pyridine modes in $Zn(py)_2Cl_2$ and in condensed pyridine and pyridine-d_5 are shown in Figs. 4 and 5, respectively. It is evident from these figures that the frequencies of ν_1, ν_{12}, and most other modes shift to the blue upon compression in pyridine and its complexes, except for ν_{6a}, ν_{6b}, and ν_{12} [the latter in $Zn(py)_2Cl_2$, phase I] which are only marginally affected by pressure. It is further evident from Fig. 5 that the internal pyridine modes do not reflect the phase transition occurring at ~20 kbar in pyridine and pyridine-d_5.[12] On the other hand, the phase transition which occurs at ~10 kbar in $Zn(py)_2Cl_2$ is clearly evident in the pressure dependence of its internal modes.

ν_1 occurs at 998 cm^{-1} in solid pyridine and its glassy modification and has a half-width of 1.2 cm^{-1}. ν_{12} occurs at 1038 cm^{-1} and has a half-width of 1.3 cm^{-1} in both modifications of solid pyridine. The pressure dependence of the half-widths of ν_1 in the crystalline and glassy modifications of pyridine are equal to 0.027 and 0.055 cm^{-1}/kbar, respectively. The respective values for ν_{12} are equal to 0.05 and 0.04 cm^{-1}/kbar. In liquid pyridine at ambient conditions ν_1 and

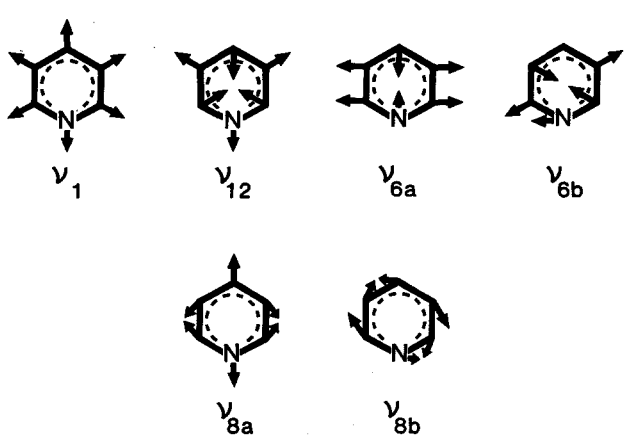

FIG. 3. A schematic representation of the ring modes ν_1, ν_{12}, ν_{6a}, ν_{6b}, ν_{8a}, and ν_{8b}.

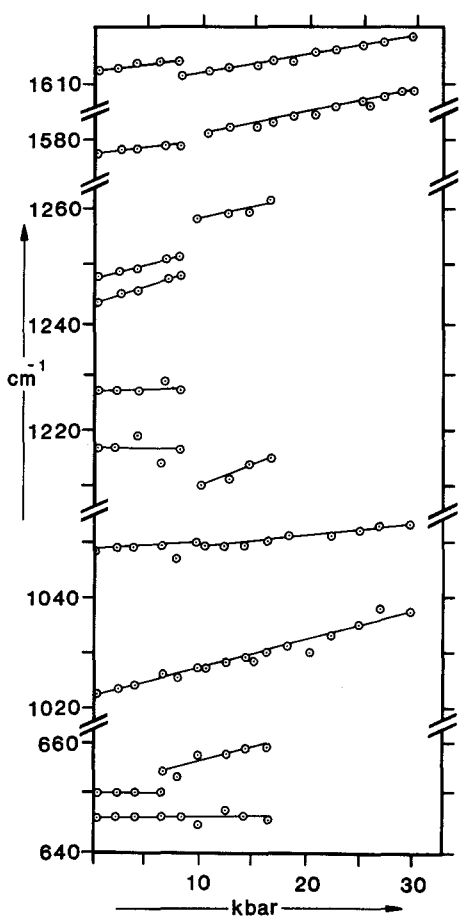

FIG. 4. The pressure dependences of some internal Raman modes in $Zn(py)_2Cl_2$. From the top, the modes are ν_{8a}, ν_{8b}, two components of ν_3, ν_{9a}, ν_{9b}, ν_{12}, ν_1, and two components of ν_6.

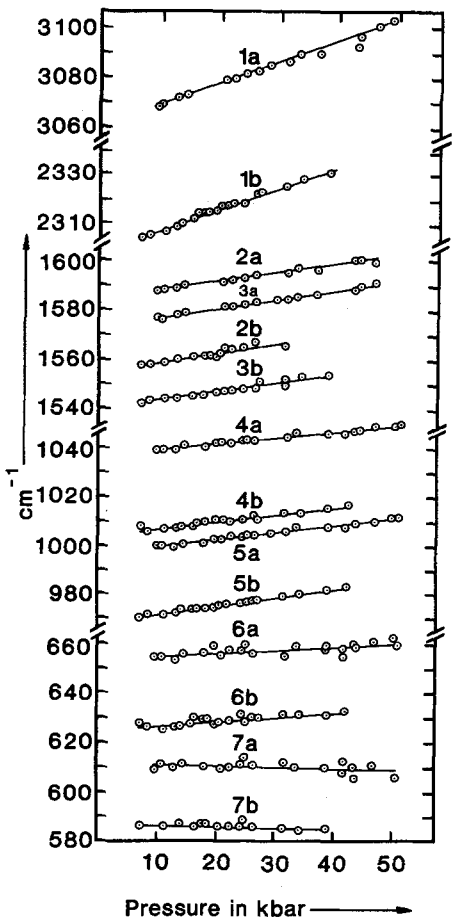

FIG. 5. The pressure dependences of some internal Raman modes in pyridine (indicated by *a*) and pyridine-d_5 (indicated by *b*). (1) ν_2 (C–H); (2) ν_{8a} (C–C ring stretch); (3) ν_{8b} (C–C ring stretch); (4) ν_{12} (ring bend); (5) ν_1 (C–C ring stretch); (6) ν_{6a} (ring bend); (7) ν_{6b} (ring bend).

ν_{12} occur at 991 and 1031 cm^{-1} and have half-widths of 3.5 and 4 cm^{-1}, respectively. The ν_1 linewidth for pyridine solutions did not show any discernible change with pressure[1] in contrast to the broadening seen in adsorbed pyridine[13] and the slight broadening observed for solid pyridine here. A considerable narrowing of these modes will take place when the liquid is frozen because of the reduced amplitude for molecular motion in the condensed phase. However, these lines are considerably broader in a 3.8 M aqueous solution of pyridine than in neat pyridine as is exemplified by the half-width of ~9.8 cm^{-1} recorded at 8 kbar, and of 5.6 cm^{-1} for the same solution frozen at 9 kbar.[1] A comparison of the latter value with those obtained for the solid in the present study shows that the half-widths do not only depend on the amplitudes of molecular motion, but are also very sensitive towards the formation of hydrogen bonds. The pressure dependences of the frequencies of ν_1 and ν_{12} in the crystalline and glassy modifications are almost identical. The assumed less regular arrangement of pyridine molecules in the crystal lattice of the glassy phase is reflected by the increase in the half-width of ν_1 compared to its value in the crystalline phase only at higher pressures. It has already been shown that different orientations of pyridine molecules adsorbed on gold surfaces give rise to a marked increase in the linewidth of ν_1.[13] The fact that the half-widths of ν_{12} and their pressure dependences are not really different in the two modifications of pyridine shows that this mode is not so sensitive with respect to the orientational order in the crystal.

The h_5–d_5 isotopic ratio of ν_1 in solid pyridine is equal to 1.0278, which is almost equal to those in the vapor, liquid, and aqueous solutions.[1, 2, 23, 24] In the case of chemisorbed pyridine, this ratio is much larger, possibly because of the fact that pyridine is bonded to the surface in such a way that the reduced mass for the ν_1 mode is affected.[13] In the case of ν_{12}, the trigonal symmetry of this mode (Fig. 3) causes it to be sensitive towards the substitution of hydrogen by deuterium in pyridine.[1, 13] This is so because the C–D mass is equal to that of N, causing the change in molecular volume during the vibration to become very small indeed in pyridine-d_5. This vibration can then almost be compared with the corresponding one in benzene of D_{6h} symmetry, which is forbidden. The intensity of ν_{12} is therefore much lower in pyridine-d_5 than in pyridine, as is evident in Fig. 6. This has also been observed elsewhere.[1, 13] A direct consequence of the small change in molecular volume during the ν_{12} vibration in pyridine-d_5 is that ν_{12} is much less pressure sensitive than in pyridine.[1] The isotopic ratio for h_5–d_5 for ν_{12} in solid pyridine was observed to be equal to 1.0318 in the present work, which is significantly higher than those published for the vapor (1.0167), liquid (1.0218), and a 1.8 M aqueous solution (1.0227).[1, 23, 24] An explanation for this is that $\partial\nu_{12}/\partial p$ is equal to 0.35 cm^{-1}/kbar for pyridine in the liquid state, compared to < 0.05 cm^{-1}/kbar for pyridine-d_5 in the liquid state. These different pressure sensitivities over a pressure range of 10 kbar (the freezing point of neat pyridine) will then certainly be reflected in the h_5–d_5 isotopic ratio.

The ratio $\partial\nu_1/\partial p$ is equal to 0.52 cm^{-1}/kbar in liquid pyridine[1] compared to the value of 0.37 cm^{-1}/kbar determined in the present study for condensed pyridine. In the complexes, these values range between 0.4 cm^{-1}/kbar for $Ni(py)_2Cl_2$ and 0.6 cm^{-1}/kbar for $Ni(py)_4Cl_2$. It was observed elsewhere[2] that hydrogen bonding increases the value of $\partial\nu_1/\partial p$, explaining the relatively high value observed in liquid pyridine where hydrogen bonds are more important than in the condensed state, as will be shown later. Any stiffening of the hydrogen-bonded network will affect the O–H- - -N bonds which, in turn, will increase the ring frequencies of pyridine.[1] The formation of M–N bonds has a dramatic effect on the frequencies of the ring modes ν_1 and ν_{12}, as can be seen in Table II, and upon further compression of these samples, the M–N bonds will be strengthened, causing a further increase in the ring frequencies of the ligand.

The frequencies of ν_1 and ν_{12} in the complexes investigated here show that those observed in $Ni(py)_4Cl_2$ are considerably lower (999, 1011, and 1037 cm^{-1}, respectively) than in the other complexes. In agreement with the structure of $Ni(py)_4Cl_2$, ν_1 is observed to be split, reflecting the two distinct pyridine groups. The lower frequencies of both ν_1 and ν_{12} could be explained in terms of the bonding from the Ni ion to the π^* orbitals of the pyridine groups and it can therefore be concluded that the C–C bonds must be weaker in $Ni(py)_4Cl_2$ than in the other complexes. A number of

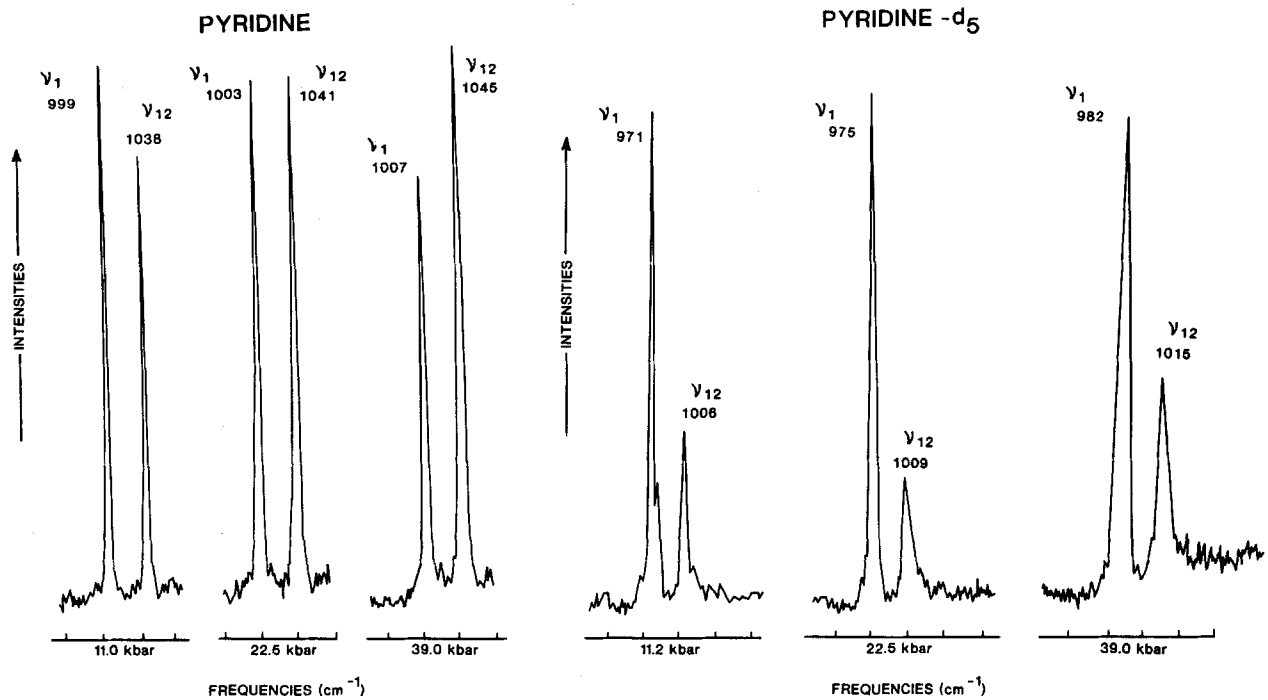

FIG. 6. The intensities of ν_1 and ν_{12} in pyridine and pyridine-d_5 at various pressures.

other internal Raman-active modes of $Ni(py)_4Cl_2$ show similar red shifts compared to their counterparts in other complexes (Table I).

The ratio of intensities of the ring modes $I\nu_{12}/I\nu_1$ is very sensitive to the strength of any N---X bonds [X = H, D, or metal (II) ions].[25] It was, e.g., found that $I\nu_{12}/I\nu_1$ decreases when pyridine is hydrogen bonded, then protonated, and finally coordinated. In a 10% pyridine solution of pyridine in CCl_4, $I\nu_{12}/I\nu_1$ is equal to 0.91 and in a 10% solution of pyridine in $CHCl_3$, which represents a hydrogen-bonded pyridine molecule, it is equal to 0.80. In a 10% solution of pyridine in water, $I\nu_{12}/I\nu_1 = 0.45$, while it varies between 0.34 and 0.15 in the pyridinium ion.[25] It is interesting to note that in liquid pyridine this ratio is equal to 0.75 compared to 0.84 in condensed pyridine at 11 kbar. Considering these intensity ratios, it can be concluded that hydrogen bonds are of less importance in the condensed phase than in liquid pyridine.

It is shown in Fig. 7 that $I\nu_{12}/I\nu_1$ varies linearly with the sample pressure in solid pyridine; this is, however, not the case in pyridine-d_5, where this ratio hardly changes upon an increase in the sample pressure. In the case of the glassy phase of pyridine, a linear plot of $I\nu_{12}/I\nu_1$ against the sample pressure is also obtained, but with a significantly higher slope than that of crystalline pyridine.

More dramatic variations take place in $I\nu_{12}/I\nu_1$ upon the coordination of pyridine. It has been reported[25] that this ratio is small upon coordination, e.g., it is equal to 0.15 in pyridine oxide and 0.05 in $Zn(py)_2Cl_2$. However, $I\nu_{12}/I\nu_1$ was determined to be equal to >0.60 in the complex $Cd(py)_2Cl_2$ in the present study, so that a generalization about this ratio of intensities in coordination compounds should be regarded with a great deal of caution. In Fig. 8, these ratios are graphically represented against $4\pi^2c^2\nu_s^2\mu$ (where ν_s is the symmetric M–N stretching mode and μ the reduced mass) for various pyridine complexes. The almost linear relationship that is obtained shows that the ratio of the intensities of these bonds depends directly on the strength of the M–N bonds. This conclusion once again emphasizes the sensitivity of the ratio of intensities $I\nu_{12}/I\nu_1$ towards N–M or N–H interactions in pyridine and its complexes.

In Fig. 9, $I\nu_{12}/I\nu_1$ values are plotted against the pressure dependence of ν_{12}, $\partial\nu_{12}/\partial p$. It is clear that a correlation exists between $\partial\nu_{12}/\partial p$ and $I\nu_{12}/I\nu_1$ in solid pyridine and its complexes. It was mentioned elsewhere that the formation of hydrogen bonds in liquid pyridine is accomplished by the

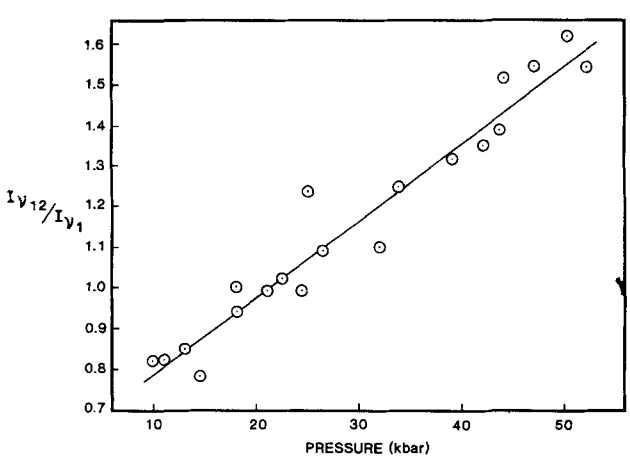

FIG. 7. The variation of the ratio of the intensities $I\nu_{12}/I\nu_1$ with pressure in pyridine.

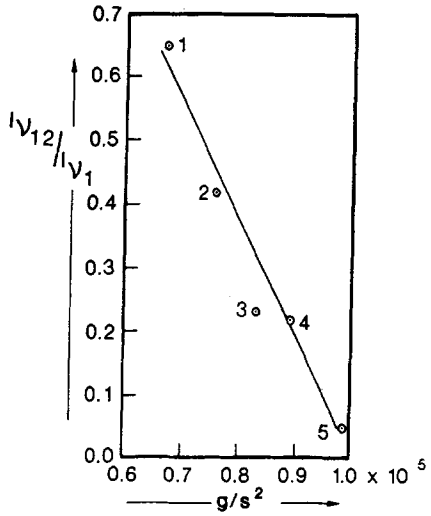

FIG. 8. The variation of the ratio of the intensities $I\nu_{12}/I\nu_1$ against $4\pi^2c^2\nu_i^2\mu$ in a series of complexes. (1) $Cd(py)_2Cl_2$; (2) $Ni(py)_2Cl_2$; (3) $Cu(py)_2Cl_2$; (4) $Ni(py)_4Cl_2$; and (5) $Zn(py)_2Cl_2$.

formation of dimers.[1] It was also shown in the previous paragraph that the intensity of ν_{12} is very much dependent on the strength of any N- - -X (X = metal, H, or D) interactions. In pyridine-d_5, ν_{12} is of low intensity as has already been shown and any further interactions involving the N atom in the formation of hydrogen bonds will weaken ν_{12} to the extent that its intensity becomes anomalously low. A low intensity of ν_{12} can be correlated with a low pressure derivative

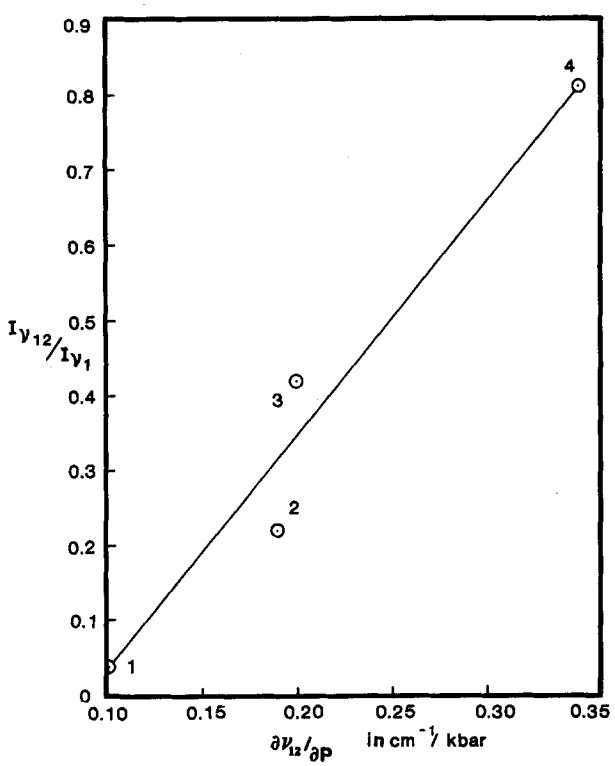

FIG. 9. The variation of the ratio of the intensities $I\nu_{12}/I\nu_1$ against the pressure dependence of ν_{12}, $\partial\nu_{12}/\partial p$, in solid pyridine and its complexes. (1) $Zn(py)_2Cl_2$; (2) $Ni(py)_4Cl_2$; (3) $Ni(py)_2Cl_2$; and (4) solid pyridine.

$\partial\nu_{12}/\partial p$. In solid pyridine-$d_5$, the intensity of ν_{12} is much lower than in pyridine, but it is certainly not negligible, as can be seen in Fig. 6. The disruption of hydrogen bonds in the condensed phase of pyridine-d_5 therefore has a marked effect on both the intensity and pressure dependence of ν_{12}. The pressure dependence of ν_{12} in solid pyridine-d_5, just as in pyridine, is dominated by intermolecular interactions, and in particular by the repulsive components of these forces. The fact that $\partial\nu_{12}/\partial p$ is virtually identical for pyridine and pyridine-d_5 in the condensed phase shows that any difference in the change of molecular volume caused by ν_{12} is pyridine and pyridine-d_5 is completely offset by intermolecular interactions in determining the size of $\partial\nu_{12}/\partial p$.

Fermi resonance occurs when two molecular vibrational modes of the same symmetry are coupled by the anharmonic part of the intramolecular function. ν_1 and ν_{12} are of the same symmetry and are typically separated by ~ 25 cm^{-1} in the complexes studied here and by 40 cm^{-1} in solid pyridine and 44 cm^{-1} in solid pyridine-d_5. These modes can therefore be expected to be coupled by Fermi resonance and a pressure-tuned Fermi resonance has indeed been reported in the solid phase of pyridine and in concentrated aqueous solutions.[1] The effect of pressure on a pair of similar neighboring vibrations can be to bring them closer together or push them apart or to alter the anharmonic coupling of the modes. It is therefore interesting to determine whether Fermi resonance in pyridine and its complexes will be enhanced or weakened by the application of pressure. If the energy levels of both ν_1 and ν_{12} shift because of Fermi resonance, the separation between the observed bands $\Delta\nu = \nu_{12} - \nu_1$ and the separation between the unperturbed frequencies $\Delta\nu^0 = \nu_{12}^0 - \nu_1^0$ can be related by

$$\Delta\nu^2 = (\Delta\nu^0)^2 + 4W^2,$$

where W is the Fermi resonance coupling. If the intensity of the unperturbed oscillator ν_{12}^0 can be assumed to be equal to approximately zero, the ratio of the intensities $I\nu_{12}/I\nu_1$ is related to $\Delta\nu$ and $\Delta\nu^0$ as follows:

$$I\nu_{12}/I\nu_1 = \frac{\Delta\nu - \Delta\nu^0}{\Delta\nu + \Delta\nu^0}.$$

If $Zn(py)_2Cl_2$ is used as an example, where the mode ν_{12} is of very low intensity, it is shown in Fig. 10 that W increases in phase II, changing abruptly at the phase transition point, then decreasing in phase I over the pressure range covered in the present study. It is also shown in Fig. 10 that the ratio $I\nu_{12}/I\nu_1$ remains almost constant in phase I, in direct contrast to its behavior in phase II. On the other hand, the frequency separation between ν_{12} and ν_1, $\Delta\nu$, decreases linearly with pressure in the whole pressure range covered in the present study, as is evident in Fig. 10. The symmetric stretching mode ν(Zn–N) increases with pressure in both phases of $Zn(py)_2Cl_2$, as is also shown in Fig. 10. Fermi resonance will enhance the intensity of ν_{12}, while on the other hand, increasingly stronger Zn–N interactions will decrease the intensity of ν_{12}. In pyridine, it is clear in Figs. 6 and 7 that the intensity of ν_{12} grows rapidly with pressure due to Fermi resonance until it is considerably more intense than ν_1 at 50 kbar. In the complexes studied here, with the exception of $Zn(py)_2Cl_2$, in phase I it was found that the

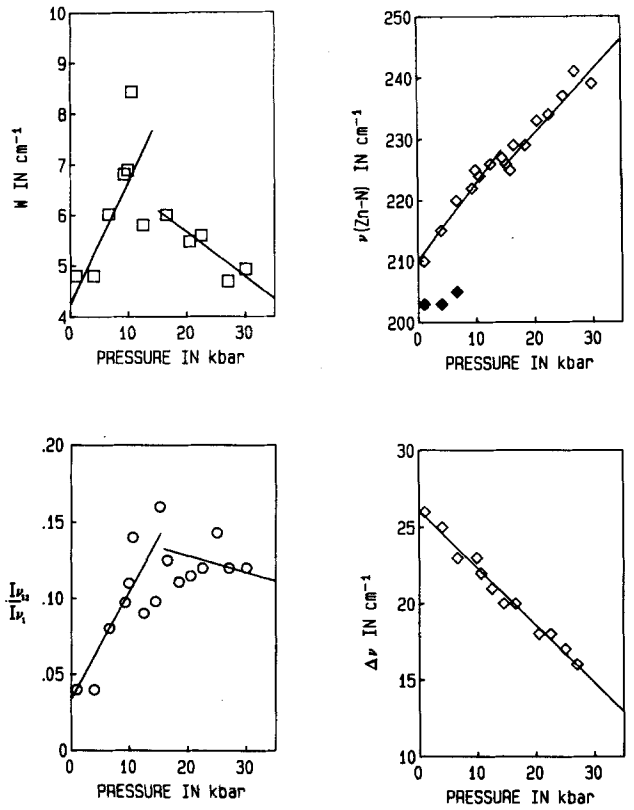

FIG. 10. The variation of (a) the Fermi anharmonic coupling constant W; (b) $I\nu_{12}/I\nu_1$; (c) ν(Zn–N); and (d) $\Delta\nu(\nu_{12}-\nu_1)$ with pressure in $Zn(py)_2Cl_2$.

increase of $I\nu_{12}/I\nu_1$, if it does occur at all, is not nearly as rapid as in the case of pyridine. This once again emphasizes the influence of M–N interactions on the ratio of $I\nu_{12}/I\nu_1$.

It was previously reported that the infrared frequencies of ν_{6a}, the in-plane bending mode which is shown with its counterpart ν_{6b} in Fig. 3, correlates with the M–N bond strength in pyridine complexes.[8] These modes are very much insensitive to pressure, although ν_{6b} showed slightly negative pressure dependences in pyridine and pyridine-d_5. In benzene, the main components of ν_6 were also reported to be insensitive towards pressure.[26] ν_{6a} shifts noticeably when pyridine is coordinated and as can be seen in Table II, shifts as large as 42 cm^{-1} have been recorded. ν_{8a} is also shown in Fig. 3 and it occurs at 1588 cm^{-1} in solid pyridine, at 1582 cm^{-1} in dried pyridine in the liquid state, and at 1593 cm^{-1} in "wet" pyridine in the liquid state.[27] In other words, this vibration is sensitive towards hydrogen bonding, but in the present study no correlation could be obtained between the bonding in the different complexes and in pyridine and pyridine-d_5 and the frequencies of ν_{8a} and ν_{8b}. It is also rather difficult to assign these modes unambiguously since the combination mode $\nu_1 + \nu_{6a,b}$ can also occur in this frequency range.

B. C–H stretching and bending modes

The C–H stretching region in gaseous pyridine is characterized by the occurrence of many fundamentals in the infrared spectra such as ν_{20a}, ν_{7b}, ν_{13}, ν_{20b}, and ν_2, in addition to combination bands such as $\nu_{8b}+\nu_{19b}$, $\nu_{8b}+\nu_{19a}$, etc.[23] Although not all of these bands are expected to be resolved in the liquid or condensed states of pyridine, complex spectra can nevertheless be expected in this frequency range. This is borne out by the experimental results of condensed pyridine shown in Fig. 1. Some of these features can be assigned to overtone and combination bands such as $2\nu_{19}$(2967 cm^{-1}), $\nu_8+\nu_{19}$(3038 cm^{-1}), $2\nu_{8b}$(3159 cm^{-1}), and $2\nu_{8a}$(3175 cm^{-1}). The bands at 3061 cm^{-1} (ν_{20a}) and 3070 cm^{-1}(ν_2) also occur in the compounds $Ni(py)_2Cl_2$ (Fig. 2), $Ni(py)_4Cl_2$, and $Zn(py)_2Cl_2$ (phase II). There can therefore be little doubt that they represent fundamental stretching modes. Upon deuteration of pyridine, these bands shift to 2300 cm^{-1}(ν_2), while the doublet at 2260/2272 cm^{-1} can possibly be assigned ν_{20a}/ν_{20b}. However, the components at 3081 and 3100 cm^{-1} in solid pyridine cannot be readily assigned to combination and/or overtone bands and most probably represent the C–H fundamentals $\nu_2(2)$ and $\nu_{20a}(2)$ of the second distinct pyridine group in the solid. (The numerals 1 and 2 are used to distinguish between the two pyridine groups.) In pyridine-d_5, the components at 2308 and 2084/2096 cm^{-1} can possibly be assigned likewise to the modes $\nu_2(2)$ and $\nu_{20a,b}(2)$ of the second pyridine group. The components observed in the Raman spectrum of glassy pyridine closely resemble those of crystalline pyridine and, in particular, give rise to well-resolved and narrow Raman bands. Furthermore, it is clearly evident in Fig. 1 that the C–H stretching modes in condensed pyridine are much less intense than those of $Ni(py)_2Cl_2$ shown in Fig. 2, where the C–H stretching modes are comparable to ν_1 in intensity. In $Zn(py)_2Cl_2$, phase II and $Ni(py)_4Cl_2$, the C–H stretching modes are also of low intensity and characterized by multiple components. As was shown earlier, there is more than one distinct pyridine group in solid pyridine and the complexes $Zn(py)_2Cl_2$ and $Ni(py)_4Cl_2$, and the C–H stretching modes in these compounds are characterized by more fundamental modes than just ν_2 and ν_{20a}, as well as by low relative intensities of these bands compared to ν_1. In $Zn(py)_2Cl_2$ phase II, three relatively weak C–H stretching modes occur at 3076, 3083, and 3086 cm^{-1} and in phase I, ν_2 and ν_{20a} occur, respectively, at 3085 and 3075 cm^{-1}. In phase I of $Zn(py)_2Cl_2$, ν_2 and ν_1 are of equal intensity. The pressure dependences of the C–H stretching modes in $Zn(py)_2Cl_2$ are shown in Fig. 11, while those of ν_2 in pyridine and pyridine-d_5 have already been shown in Fig. 5. The most intense C–H stretching mode ν_2 has a pressure dependence of 0.84 ± 0.16 cm^{-1}/kbar in all compounds where only one type of pyridine group is found; ν_{20a} is the weaker component which appears as a satellite on the main component and is much less pressure sensitive than ν_2 with $\partial\nu_{20a}/\partial p = 0.53 \pm 0.10$ cm^{-1}/kbar in all the compounds studies here. The C–H stretching mode in $Zn(py)_2Cl_2$ phase II can therefore be assigned as follows: $\nu_2(1)$ at 3076 cm^{-1} ($\partial\nu_2/\partial p = 0.82$ cm^{-1}/kbar); $\nu_{20a}(1)$ at 3083 cm^{-1} ($\partial\nu_{20a}/\partial p = 0.43$$cm^{-1}$/kbar; and $\nu_2(2)$ at 3086 cm^{-1} ($\partial\nu_2/\partial p = 1.27$ cm^{-1}/kbar). The two C–H stretching bands that occur 3075 and 3085 cm^{-1} at 10 kbar

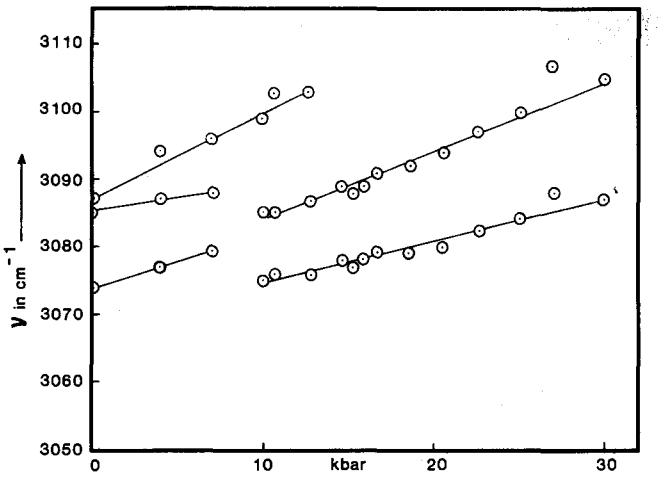

FIG. 11. The pressure dependences of the C–H stretching modes in $Zn(py)_2Cl_2$.

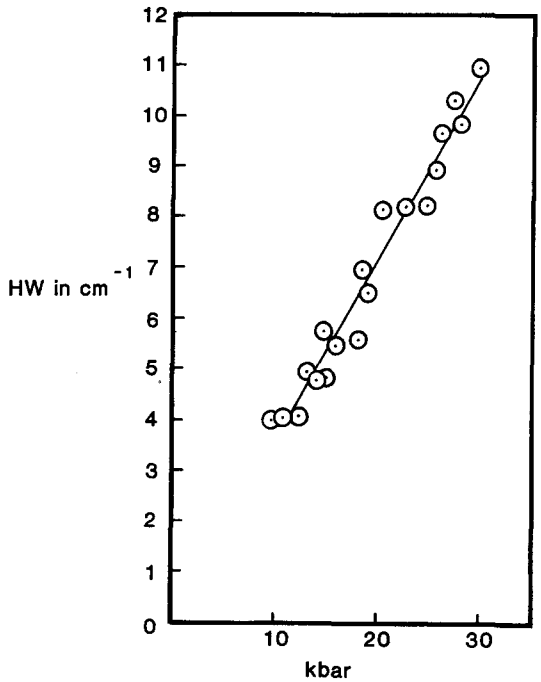

FIG. 12. The pressure dependence of the half-width (HW) of the C–H stretching mode ν_2 in $Zn(py)_2Cl_2$ phase I above 10 kbar.

in $Zn(py)_2Cl_2$(II) are very similar in appearance to the ones shown in Fig. 2 for $Ni(py)_2Cl_2$.

The C–H stretching modes can now also be assigned in solid pyridine and pyridine-d_5, as has been done in Table I. In $Ni(py)_4Cl_2$, two prominent modes are observed at 3075 and 3054 cm^{-1}. A weak shoulder occurs at 3067 cm^{-1}. The pressure dependences of these two bands are very similar (Table I) and are therefore assigned to $\nu_2(1)$ and $\nu_2(2)$, respectively. The shoulder is assigned to $\nu_{20a}(1)$.

From these results, it can be concluded that the C–H stretching modes in these solids appearing in the Raman spectra are confined to ν_2 and ν_{20}. They do reflect the presence of more than one distinct pyridine group in the lattice, but they are not sensitive towards long-range order in the crystals, judging from the similarity of the Raman spectra of the glassy and crystalline modifications of pyridine. No evidence could be found in the pressure dependence of the Raman spectra of the existence of strong hydrogen bonds in these solids, even though the existence of inter- and intramolecular hydrogen bonds was suggested in the crystal structure analysis of $Zn(py)_2Cl_2$ phase II.[17] In $Ni(py)_4Cl_2$, $\nu_2(2)$ which occurs at 3054 cm^{-1} seems to suggest a weaker C–H bond which could be the result of some hydrogen bonding, however, the pressure dependence of this bond rules out any strengthening of the bonds at higher pressures. Hydrogen bonding in this complex can be explained in terms of the d_π-electron delocalization between the nickel (II) ion orbitals and the π electrons of the pyridine rings. It has been observed in $Cu(py)_4Cl_2$ dissolved in protic solvents that the d_π-electron delocalization within the complex and the H– – –π type of interaction of the complex with the protic solvent are cooperative, mutually enhancing each other.[28] It is therefore possible that H– – –π interactions can also occur in $Ni(py)_4Cl_2$ in the solid state.

The C–H stretching modes are pressure sensitive with respect to both frequencies and half-widths. The variation of the half-width of ν_2 in $Zn(py)_2Cl_2$ phase I is shown in Fig. 12. The half-width of ν_2 increases at a rate of 0.37 cm^{-1}/kbar and this, in addition to the significant pressure dependence of the frequency of this band of 1 cm^{-1}/kbar, shows that the repulsive components of the intermolecular forces become increasingly important at higher pressures. The same is true of the C–H stretching modes in other complexes as well as in pyridine and pyridine-d_5. The pressure dependence of the half-widths of ν_2 can be compared with that of ν_1, mentioned earlier. It is evident that the C–H modes are much more sensitive to intermolecular interactions than, e.g., the C–C ring mode ν_1. The association of the pyridine molecules in the condensed state does not occur because of the formation of hydrogen bonds since the effect of pressure will undoubtedly be to strengthen such N– – –H bonds, which will lead to a decrease in the strength of the C–H bonds resulting in a red shift in the frequencies of these modes.

DiLella and Stidham[24] carefully studied the Raman spectra of pyridine and its deuterated analogous such as pyridine-4*d*, pyridine 2, 6-d_2, pyridine 2, 4, 6-d_3 and these data, in addition to those of pyridine and pyridine-d_5 (which were already known), made a complete assignment of the pyridine vibrations in the liquid state possible. The frequencies of the modes ν_2, ν_{13} and ν_{20a} coincide in liquid pyridine (occurring at 3057 cm^{-1}), while ν_{7a} occurs at 3042 cm^{-1} and ν_{20b} at 3079 cm^{-1}. This means that ν_2 shifts downwards from 3094 to 3079 cm^{-1} in going from the vapor to the liquid states, ν_{20b} from 3087 to 3079 cm^{-1}, ν_{13} from 3073 to 3057 cm^{-1}, while ν_{20a} shifts from 3030 to 3057 cm^{-1} (the vapor values are from the infrared measurements[23]). It therefore appears as if a weakening of the C–H bonds occurs in the liquid, which could be indicative of the formation of hydrogen bonds in the liquid state. It was previously reported[1] that the *ortho*, and to a lesser extent the *para* C–H bonds of pyridine show appreciable acidic character and can therefore

form hydrogen bonds. At the liquid to solid transition in pyridine, many of the C–H stretching modes shift upwards, e.g., ν_2 from 3057 to 3070 cm^{-1}, etc. These shifts are most probably indicative of a disruption of the hydrogen bonds in the solid state.

The in-plane H bending modes ν_3 and ν_{9a} and ν_{9b} occur at 1233 and 1213 (ν_{9a} and ν_{9b}), respectively, in solid pyridine. In $Zn(py)_2Cl_2$(II), these bands occur at 1243/1247 cm^{-1} (ν_3) and 1217/1226 cm^{-1} (ν_{9a} and ν_{9b}) as can be seen in Fig. 4. The splitting of ν_3 disappears at the phase transition and the ν_3 is observed as a single band at 1258 cm^{-1}. A very slight splitting of ν_9 into two components at 1209/1211 cm^{-1} is observed immediately above the phase transition, but this soon disappears at higher pressures. In $Ni(py)_4Cl_2$, ν_9 occurs at a single component at 1217 cm^{-1} and ν_3 at 1235 cm^{-1} as a broad and very weak feature. In $Ni(py)_2Cl_2$, ν_9 occurs at 1231 cm^{-1} as a band of medium intensity and ν_3 occurs at 1243 cm^{-1} as a very weak component (Fig. 2). The pressure dependences of these weak bands could not always be followed accurately in the high-pressure cell. However, both ν_3 and ν_9 are rather pressure sensitive in pyridine, the same applies to ν_3 in $Zn(py)_2Cl_2$ with $\partial\nu_3/\partial p = 0.67\ cm^{-1}$/kbar, however, the two components of ν_9 show virtually no pressure dependence. In phase I of $Zn(py)_2Cl_2$, both ν_3 and ν_9 are once again very much pressure sensitive.

V. CONCLUSION

The intermolecular forces in solid pyridine and pyridine-d_5 do not involve strong hydrogen bonds and are most probably of a polar nature. An analysis of the pressure dependence of the C–H stretching modes in pyridine and its complexes shows that the repulsive components of these intermolecular forces dominate at higher pressures. The C–H stretching modes, or as a matter of fact all other internal modes, are not very sensitive towards the positional order of the pyridine rings in the crystal investigated here. The C–H stretching modes do reflect the presence of more than one distinct pyridine group in the lattice.

Fermi resonance occurs between the ring modes ν_1 and ν_{12} in pyridine and its complexes, and in the case of $Zn(py)_2Cl_2$(II), a linear increase is observed in the Fermi resonance coupling constant W with pressure, accounting for the progressive increase in the intensity of ν_{12} with pressure. The same applies to, e.g., $Ni(py)_2Cl_2$, where a linear relationship was obtained between $\Delta\nu = \nu_{12} - \nu_1$ and the sample pressure, resulting in an increase in the intensity of ν_{12} with pressure. The reason why Fermi resonance is not important in liquid pyridine-d_5 is that the change in molecular volume during ν_{12} is very small because of the equal C–D and N masses and furthermore, the hydrogen bonds existing in liquid pyridine-d_5 contribute towards a very low intensity of ν_{12}. The combined effect of these factors is an anomalously low intensity for ν_{12} in the liquid state and virtually no Fermi resonance coupling. In solid pyridine-d_5, the intensity of ν_{12} has increased due to a disruption of hydrogen bonds, but no direct correlation could be obtained between the ratio of intensities $I\nu_{12}/I\nu_1$ and pressure, or between the frequency separation ν_{12}–ν_1 and pressure and it must be concluded that Fermi resonance is weak here too, or even completely absent.

The influence of the strength of any N– – –X (X = H, D, or metal ion) interaction in pyridine and its complexes on the intensity of ν_{12} is the most important result obtained in the present study. A comparison of the relative Raman intensities of ν_{12} and ν_1 in a series of pyridine complexes shows that one can immediately relate the ratio of intensities $I\nu_{12}/I\nu_1$ to the strength of the M–N bond. This also influences the pressure derivative $\partial\nu_{12}/\partial p$ which is related to the ratio of intensities $I\nu_{12}/I\nu_1$. In one of the complexes investigated here [$Ni(py)_4Cl_2$], evidence was found of d_π delocalization within the complex, however, the pressure dependence of the Raman bands of this complex was no different from that of the other complexes and therefore does not point to an increase in this delocalization with pressure. Any such interaction will involve a d_π-electron delocalization from the nickel ion to the π^* orbitals of the coordinated pyridine groups, weakening the bonding in the ring. In $Cu(py)_4Cl_2$, where similar interactions are known to occur, the complex decomposed spontaneously to $Cu(py)_3Cl_2$,[28] however, our high-pressure Raman spectra gave no indication of such behavior in $Ni(py)_4Cl_2$.

ACKNOWLEDGMENTS

We thank Sastech, Sasolburg for supporting this project financially. We are also grateful to the Council of the University of Pretoria and the Foundation for Research Development, Pretoria for financial support.

[1] M. R. Zakin, S. G. Grabb, H. E. King, Jr., and D. R. Herschbach, J. Chem. Phys. **84**, 1080 (1986).
[2] M. R. Zakin and D. R. Herschbach, J. Chem. Phys. **85**, 2376 (1986).
[3] J. E. Demuth, P. N. Sandra, J. M. Warlaumont, J. C. Tsang, and K. Christmann, in *Vibrations at Surfaces*, edited by R. Caudano, J. -M. Gilles, and A. A. Lucas (Plenum, New York, 1982), pp. 391–411.
[4] M. Moskovits and D. P. DiLella, in *Surface Enhanced Raman Scattering*, edited by R. K. Chang and T. E. Furtak (Plenum, New York, 1982), pp. 243–273.
[5] N. S. Gill, R. H. Nuttall, D. E. Scaife, and D. W. A. Sharp, Inorg. Nucl. Chem. **18**, 79 (1961).
[6] M. W. Venter and A. M. Heyns, Inorg. Chem. **26**, 1095 (1987).
[7] M. Goldstein and W. D. Upsworth, Spectrochim. Acta Part A **28**, 1107 (1972).
[8] M. Suzuki and W. J. Orville-Thomas, J. Mol. Struct. **37**, 321 (1977).
[9] J. E. Rüede and D. A. Thornton, J. Mol. Struct. **34**, 75 (1976).
[10] S. Akyüz, A. B. Dempster, R. L. Morehouse, and S. Suzuki, J. Mol. Struct. **17**, 105 (1973).
[11] W. Libus, S. K. Hoffmann, M. Kluczkowski, and H. Twardowska, Inorg. Chem. **19**, 1625 (1980).
[12] A. M. Heyns and M. W. Venter, J. Phys. Chem. **89**, 4546 (1985).
[13] C. J. Sandroff, H. E. King, Jr., and D. R. Herschbach, J. Phys. Chem. **88**, 5647 (1984).
[14] P. T. T. Wong, J. Chem. Phys. **63**, 5108 (1975).
[15] J. J. Kim, G. Salvador, and W. F. Sherman, in *Proceedings of the XIth International Conference on Raman Spectroscopy*, edited by R. J. H. Clark and D. A. Long (Wiley, Chicester, 1988), pp. 481–482.
[16] D. Mootz and H. G. Wussow, J. Chem. Phys. **75**, 1517 (1981).
[17] W. L. Steffen and G. J. Palenik, Acta Crystallogr. Sect. B **32**, 298 (1976).
[18] A. M. Heyns. (to be published).
[19] B. Morosin, Acta Crystallogr. Sect. B **31**, 632 (1975).
[20] V. H. Paulus, Z. Anorg. Allg. Chem. **369**, 38 (1969).
[21] M. A. Porai-Koshits, Kristallografiya **5**, 605 (1960).

[22]K. F. Purcell and J. C. Kotz, *Inorganic Chemistry.* (Saunders, London, 1977).
[23]V. A. Walters, D. L. Snavely, S. D. Colson, K. B. Wiberg, and K. N. Wong, J. Phys. Chem. **90**, 592 (1986).
[24]D. P. DiLella and H. D. Stidham, J. Raman Spectrosc. **9**, 90 (1980).
[25]A. Campion, in *Vibrational Spectroscopy of Molecules on Surfaces*, edited by J. T. Yates, Jr. and T. E. Madey (Plenum, New York, 1987), Chap. 5, pp. 397–398.
[26]M. M. Thiéry and J. M. Léger, J. Chem. Phys. **89**, 4255 (1988).
[27]D. P. DiLella and H. D. Stidham, J. Raman Spectrosc. **9**, 247 (1980).
[28]W. Libus, S. K. Hoffman, M. Kluczkowski, and H. Twardowska, Inorg. Chem. **19**, 1625 (1980).